**Title**
STRUCTURE AND PROPERTIES OF ALLOYS CONTAINING VERY SMALL ORDERED PARTICLES



**Authors**
Gaudig, W.
Okamoto, P.
Schanz, G.
et al.

**Publication Date**
1969-09-01

Submitted to Trans. AIME

UCRL-19122
Preprint



c.2

# STRUCTURE AND PROPERTIES OF ALLOYS CONTAINING VERY SMALL ORDERED PARTICLES

W. Gaudig, P. Okamoto, G. Schanz, G. Thomas, and H. Warlimont

September 1969

AEC Contract No. W-7405-eng-48



LAWRENCE RADIATION LABORATORY
UNIVERSITY of CALIFORNIA BERKELEY

UCRL-19122

c.2

## DISCLAIMER

UCRL-19122

# STRUCTURE AND PROPERTIES OF ALLOYS CONTAINING VERY SMALL ORDERED PARTICLES†

W. Gaudig,* P. Okamoto, G. Schanz,* G. Thomas, and H. Warlimont*

Inorganic Materials Research Division, Lawrence Radiation Laboratory
Department of Materials Science and Engineering, University of California, Berkeley, California

These studies were initiated in order to determine whether the diffraction effects and property changes in alloys ascribed to short range order (SRO) are accompanied by microstructural features which can be resolved by transmission electron microscopy and field ion microscopy (FIM). Such features were expected to exist in the alloys concerned because several diffraction effects[1-12] and macroscopic property changes[11-19] indicate the presence of discrete ordered regions in a random matrix. In previous work short range order has been treated from two different points of view: statistical treatments are concerned with the average deviation of the numbers of like and unlike atom pairs from a random distribution; the particle concept is based upon the presence of small ordered regions in a random matrix i.e. a nonrandom distribution of like and unlike atom pairs. Among the previous observations, diffraction and electrical resistivity measurements are most relevant for discerning between these two concepts. X-ray and electron diffraction yield broadened maxima at superlattice positions of a stable phase in the same system or at different positions, in Cu-Al,[1-4,33] Fe-Al[5-7] and Ni-Mo.[8-9,11,39] The fact that the positions of superlattice reflections and SRO maxima do not coincide in some cases, e.g. in the Ni-Mo, Au-Cr, and Au-Mn systems, has been interpreted as proof for the absence of ordered particles in a random matrix.[44]

---

*Max-Planck-Institut für Metallforschung, Stuttgart, Germany

†Presented at the Bolton Landing Conference of the AIME, September 1969

The conclusion appeared to be supported by the agreement between the experimental finding of extra SRO maxima and their theoretical prediction by Clapp and Moss.[47] But this correlation will have to be reinvestigated in view of the present results. Resistivity changes exhibit an anomalous increase (i-effect), which commonly arises during early stages of precipitation due to particles of a critical size for electron scattering[20-25] in Cu-Al,[4,13-17] Fe-Al,[18-19] and Ni-Mo.[11-12,48]

The phase equilibria and the regions associated with effects of short range order are shown in Figs. 1a-d in the range of present interest for the Cu-Al,[26,27] Cu-Zn,[29,45,46] Fe-Al[18,28] and Ni-Mo[29] systems. The regions of SRO have been derived from the temperature and composition dependence of macroscopic property changes and thermal effects. The structures of the superlattice phases whose regions of stability border on the regions of SRO are: an f.c.c.-based long-period superlattice structure in Cu-Al,[4] the b.c.c.-based $DO_3$ type structure in Fe-Al[30] and an f.c.c.-based tetragonal $Dl_a$ type structure in Ni-Mo.[31]

## EXPERIMENTAL PROCEDURE

The alloys were induction melted (Cu-Al, Cu-Zn, Fe-Al) and arc melted (Ni-Mo), respectively, using metals of 99.9% (Ni), 99.99% (Al, Mo, Zn) and 99.99% (Cu) purity. 0.15% Ti was added to the Fe-Al alloys prepared for mechanical property measurements in order to minimize the effect of interstitial impurity solutes.[40] Most heat treatments were conducted under vacuum or inert gas (Ar, He) atmospheres. Isothermal annealing of the Ni-Mo alloy was carried out in a chloride salt bath. Specimens for electron microscopy were prepared by electropolishing in an electrolyte consisting of 1 part nitric acid and 2 parts methyl alcohol.

Polishing conditions were: 5 to 6V, -5 to -15°C for Fe-Al; 7V, -35 to 70°C for Cu-Al. Similar polishing procedures were employed for the Cu-Zn alloys on which preliminary results are reported. Specimens of Ni-Mo for both electron micrsocopy and FIM were prepared from the same heat treated sample. Tensile tests were performed on specimens 0,2 mm thick, whose gauge length of 30 mm was 3 mm wide at a strain rate of $10^{-4}$ $sec^{-1}$. Each state was tested on at least two specimens.

## RESULTS

### Microstructures and Electron Diffraction

In all alloys studied thus far electron microscopic bright and dark field images of foils oriented for two-beam scattering of fundamental reflections exhibit very finely dispersed contrast effects which can be interpreted in terms of a profusion of weak localized strain fields which develop to the so-called "tweed pattern" characteristic of alloys containing coherent precipitates if the volume fraction and coherency strains exceed certain values.[49,50,51,68] These features are shown in Figs. 2a-d for Cu-Al, Cu-Zn, Fe-Al and Ni-Mo alloys. In cases where single black-white images typical of small strain centres[41-43] are observed the intensity distribution is no unique and simple function of the operative diffraction vector $\vec{g}$. This indicates that neither a direction of maximum displacements nor a unique shape effect are common to all or groups of the strain centres visible.

However, some information regarding the array and the average distance of the strain centres may be derived from micrographs such as shown in Figs. 2a-d. In particular in Fe-Al alloys the net strain contrast exhibited an alignment in rows predominately in $\langle 110 \rangle$, but also in $\langle 100 \rangle$ directions depending on the foil normal and on the operating reflection.

The average distance D of these rows was found to be independent of alloy concentration and aging time within the accuracy of measurement in alloy containing 15.5 to 17.8 at. % Al aged for 1 to 170 hours, and amounted to $100 - D - 200$ Å. A count of individual strain centres in Cu-Al alloys containing 10 and 15 at. % Al, where the visibility criteria derived for vacancy clusters[43] were taken into account, yielded an average distance $D \simeq 130$A.

In all alloys investigated in the state of a high degree of SRO additional reflections are observed which allows direct dark-field images to be produced of the regions from which these extra reflections originate. They show small particles whose dispersion corresponds to the average distance of the strain centres which was derived indirectly from the strain contrast images. Examples are given in Figs. 3a and 3b. This now should enable the average particle size and number per unit volume to be measured if their visibility and geometric relations[52,53] are taken into account.

FIM images of the as-quenched $Ni_4Mo$ alloy exhibit many bright clusters containing an average of about 8 atoms each, Fig. 4a. These clusters are distributed randomly and are plate shaped with a thickness of one or two atom layers. Aging at 650°C leads to an increase in the average size of the clusters and to a decrease in number per unit area. After 10 minutes of aging, Fig. 4b, the bright clusters are definitely corresponding to small ordered regions since they appear most frequently in the form of half-rings especially in areas of the FIM image where superlattice planes would normally appear in the fully ordered alloy. The matrix of the as-quenched alloy appears to be partially ordered. The FIM ring pattern development varies from region to region with no distinct separation of such regions by an interface. The most prominent feature

of electron diffraction of the short range ordered alloys is an intense directional broadening of all fundamental reflections as shown in Figs. 5a-c. The length of the streaks increases approximately proportional to the length of the reciprocal lattice vector $\vec{g}$ thus indicating that they are predominantly due to anisotropic lattice strains.

Table 1 gives the direction of streaking observed in the different alloys. In all cases the streaks are most intense at slight deviations from low-index zones corresponding to a sharply directional propagation in reciprocal space such that their contact with the reflecting sphere is a sensitive function of orientation. It has been discussed by L. E. Tanner [54] that streaks may be prominent in <110> in f.c.c. alloys if elastic anisotropy is a main factor in determining the displacements.

As indicated above the diffraction patterns contain extra reflections whose intensity increases with increasing solute content and degree of short range order. In Fe-Al alloys, the extra reflections correspond to the $DO_3$ superlattice structure, Fig. 6a. In Cu-Al alloys, Fig. 6b, the extra reflections are compatible with a periodic modulation of the scattering amplitude in cube directions whose period was found to vary as a function of composition.[4] At 17 at. % Al the period is $L \simeq 1.6\ a$, where a is the lattice parameter of the f.c.c. unit cell. The stable superlattice at c > 19.5 at. % Al is characterised by two values of L : $L_1 = a$ and $L_2 = 2a$.[4] In Ni-Mo alloys two types of additional reflections occur. Intense spots at {1,1/2,0} positions in as-quenched specimens and very weak superlattice reflections of the $Ni_4Mo$ structure which do not lie precisely at their equilibrium angular positions. With aging the intensity of the {1,1/2,0} reflections decreases while the intensity of the the superlattice reflections increases and they are shifted to equilibrium

positions, see Fig.s 7a-c. The presence of the {1,1/2,0} maxima is compatible with periodic modulations in the direction of 420 plane normals with a period $L = 4d_{420}$. The increase in intensity and slight shifting of the superlattice reflections into their final positions in the immediate vicinity of the {1,1/2,0} spots corresponds to the growth of local regions with $L = 5d_{420}$ modulations of the scattering amplitude. This value arises because in the $Ni_4$ Mo structure every fifth {420} type plane is occupied by Mo atoms only, the intervening planes consisting of Ni atoms.

It should be noted that in as-quenched $Ni_4$ Mo the diffuse superlattice maxima corresponding to $L = 5d_{420}$ are visible only in certain reciprocal lattice sections such as {130}* which contain superlattice positions but no {1,1/2,0} positions. In {002}* sections all superlattice maxima are obscured by neighbouring {1,1/2,0} spots, whereas in other sections such as {121}* only half of the superlattice maxima are directly observable; the others are detectable only by microphotometric measurements. This explains why neither previous investigators of SRO in Ni-Mo nor L. E. Tanner et. al.[44] in investigating the corresponding Au-Mn and Au-Cr systems have reported such maxima earlier since their diffuse scattering experiments have been confined almost exclusively to {002}* reciprocal lattice sections. A detailed interpretation of these observations will be published separately.[55]

Mechanical Properties

Fe-Al alloys containing $3.0 < c < 18.1$ at.% Al were investigated after quenching from 800°C and after additional aging for 40 hours at 250°C. Characteristic stress-strain curves are reproduced in Fig. 8. Significant differences resulting from the thermal treatments were obtained

only at c > 16.0 at. % Al, the yield stress being raised about 1.5 $kgf/mm^2$ at 16.0 at. % Al and about 5 $kgf/mm^2$ at 18.1 at. % Al by the aging treatment. The yield stress in terms of the 0.1% proof stress $\sigma_{0.1}$ as a function of composition and heat treatment is plotted in Fig. 9. Some of the alloys containing 10 to 16 at. % Al exhibited discontinuous yielding. Three stages of work hardening may be distinguished in accordance with other investigations of ordered alloys:[66-68] an initial stage of zero work hardening (I) is followed by a stage of constant rate (II) and a final stage (III) of a roughly parabolic rate of work hardening. Stage I is hardly developed in the polycrystalline specimens employed for these experiments.

## DISCUSSION

### The Nature of Short Range Order

The microstructural observations and diffraction results obtained in these studies have shown that for the investigated systems the description of the state of short range order by local order coefficients alone is incomplete. Rather, it is found that discrete highly ordered regions in a matrix with lower or zero degree of order can be distinguished.

The crystal structures of the ordered regions are either identical or closely related to the stable superlattice structures occurring at higher solute contents or lower temperatures, but the degree of order in the particles is unknown. It is interesting to note that in both the Cu-Al and Ni-Mo systems the essential difference between the structural features of the small ordered regions in the state of short range order and the neighbouring superlattice phases is given by a difference in lattice periodicity. In the case of short range ordered Cu-Al a periodic scattering with $\bar{L} = 1.6a$ was observed. The reflections were weak and

diffuse, thus indicating that the extra reflections arise from quasi-periodic fluctuations of scattering whose average period is $\bar{L} = 1.6a$. The long period shift structure of the $\alpha_2$ superlattice phase consists of 6 antiphase shifts at regular intervals in 8 f.c.c. unit cells corresponding to $L = 1.33a$. In the case of Ni-Mo the {1,1/2,0} reflections can be interpreted as being due to every fourth {420} type plane (referred to the f.c.c. unit cell) yielding periodic variations in scattering, possibly because of an enrichment in Mo atoms, whereas the unit cell of the $Ni_4Mo$ structure requires periodic interactions extending as far as five of the {420} type planes of the $Ni_4Mo$ structure, because every fifth plane of this type is occupied by Mo atoms.

Electron diffraction patterns of short range ordered Au-Mn and Au-Cr alloys taken at temperature[44] exhibit the same {1,1/2,0} type maxima as those observed for Ni-Mo, but no dark field images have been published. From the results of this work and of[9] it appears that even though the structures of short range and long range order are different, the short range ordered state may, still, consist of small ordered regions in a less or disordered matrix. It should be noted that a linearized approximation for the correlation functions of binary alloys[47] yields the same type of scattering in short range ordered $Ni_4Mo$ as that found experimentally. The compatibility of the theoretical treatment with the observed presence of discrete ordered regions is still to be investigated.

The size of the ordered regions has been observed to approach a small, finite (equilibrium) value depending on aging temperature and alloy concentration.[4,7] The diameter D has been determined by several direct and indirect observations, calculations and conclusions. In

Cu-Al alloys[4] the width of x-ray reflection yields D = 21 Å, resistivity measurements lead to approximately 10 < D < 20 Å. In Fe-Al alloys[7] an approximate evaluation of the microstructure yields D < 70 Å, other authors[16] report D = 50 Å, whereas resistivity measurements indicate 10 < D < 20 Å. The FIM images of Ni-Mo yield D ≃ 12 Å; based on electron microscopy[9,37] D ≃ 10 Å has been reported.

Several previous investigations of other alloys systems have also shown that in the short range ordered state discrete ordered regions exist in a nearly random matrix, e.g., in $Cu_3Au$,[56,58] CuAu,[57] CuAu,[60] $Cu_3Pd$.[59] It is therefore concluded that these features are characteristic of the state of short range order in numerous alloys systems.

Mechanical properties measured in the present study have been analysed in terms of current theories of strengthening in connection with the observed microstructures. The plot of the yield stress as a function of concentration and heat treatment, Fig. 9, suggests that up to approximately 10 at. % Al a single functional relationship prevails which can be related to solid solution strengthening whereas at higher solute contents contributions due to short range order can be resolved. Applying the Fleischer theory for solid solution strengthening[61, 62] in its form found to hold for b.c.c. solid solutions[38] it can be shown that below 10 at. % Al the relation $\sigma_{0.1}(c_{Al})$ is well represented for screw dislocations. By extrapolating this relation to higher Al contents approximate values for the contribution due to short range order can be derived if they are assumed to be additive. This contribution was analysed in terms of the following theories of strengthening: 1.) short range order strengthening,[34, 36] 2.) strengthening due to the stress field of particles,[63,64] 3.) strengthening due to ordered misfit-free particles.[65] 1.) and 2.) yield values compatible with the experimental

findings whereas 3.) results in theoretical predictions which are smaller than the experimental values by a factor of about $10^3$, which was to be expected in view of the observed coherency strains.

Preliminary electron microscopic observations of the dislocation arrangement after different amounts of plastic deformation support the justification for subdividing the stress-strain curves into three etages. In grains suitable oriented to the tensile axis slip is restricted to few widely spaced (.$10^4$ Å) {110} slip planes in stage I. Distinctly straight screw dislocations along <111> directions are found in stage II and it appears that they are locked as dipoles due to the interaction of their strain fields as proposed by Taylor in his theory of work hardening;[69] their annihilation by cross-slip being restrained due to the ordered regions. In stage III the dislocations are still mainly straight and parallel to <111>, but in all grains slip on at least two systems and pronounced interlocking has occurred. All of these observations are similar to those by G. E. Lakso and M. J. Marcinkowski[67] on ordered Fe-Si alloys. A full account of this part of our study will be published elsewhere.[70]

## CONCLUSIONS

In the short range ordered Cu-Al, Cu-Zn, Fe-Al and Ni-Mo alloys electron and field ion microscopy and diffraction effects indicate the presence of discrete ordered regions in a less ordered or disordered matrix. It is possible to reinterpret and correlate previous observations with these findings. Since diffraction studies of several other alloy systems yield corresponding results it is suggested that a coherent two-phase mixture in which coarsening of the ordered phase is limited to a small equilibrium particle size is frequent if not common in short

range ordered alloys.

The yield stress and work hardening behaviour of short range ordered Fe-Al alloys are compatible with their structural features.

ACKNOWLEDGEMENT

We wish to thank the United States Atomic Energy Commission for making collaboration in part of this work possible at Berkeley. We also thank Mrs. M. Hage, Mrs. H. Kolbe, Miss M. Robson, L. Bitzek and D. Jurica for help with the experimental work.

## REFERENCES


1. R. G. Davies and R. W. Cahn, Acta. Met. 10 (1962) 170.
2. C. R. Houska and B. L. Averbach, J. Appl. Phys. 30 (1959) 1525.
3. B. Borie and C. J. Sparks, Acta. Cryst. 17 (1964) 827.
4. W. Gaudig and H. Warlimont, Z. f. Metallkunde 60 (1969) 488.
5. R. G. Davies , J. Phys. Chem. Solids 24 (1963) 985.
6. D. Watanabe, H. Morita, H. Saito and S. Ogawa, J. Phys. Soc. Jap. 25 (1968) 293.
7. H. Warlimont and G. Thomas, to be published in Met. Sci. J.
8. J. E. Spruiell and E. E. Stansbury, J. Phys. Chem. Solids 26 (1965) 811.
9. E. Ruedl, P. Delavignette and S. Amelinckx, phys. stat. sol. 28 (1968) 305; IV. Europ. Conf. Electron Micr., Rome, 1968, Vol. I, p. 311.
10. G. Thomas, J. Austral. Inst. Met. 8 (1963) 80.
11. H. G. Baer, Z. Metallkde. 56 (1965) 79.
12. A. N. Dubrovina and Ya. S. Umanskii, Jzv. Vyšš. Učeb. Zav. Černn. Metallurg. (1966) 140.
13. A. van den Beukel, P. C. J. Coremans and M. M. A. Vrijhoff, phys. stat. sol. 19 (1967) 177.
14. M. S. Wechsler and R. H. Kernohan, Acta Met. 7 (1959) 599.
15. V. Ye. Panin, E. K. Zenkova and V. P. Fadin, Phys. Met. Metallogr. 13, 1 (1962) 76.
16. S. Radelaar, J. Phys. Chem. Solids, 27 (1966) 1375.
17. W. Koster and H.-P Rave, Z. f. Metallk. 52 (1961) 158.
18. H. Thomas, Z. f. Metallk. 41 (1950) 185.
19. H. Saito and H. Morita, J. Jap. Inst. Met. 30 (1966) 930 (in Japanese); Sci. Rep. Res. Inst. Tōhoku Univ. A 18, Suppl. (1966) 70 (in English).

20. H. Thomas, Z. Physik 129 (1951) 219.

21. E. A. Starke, V. Gerold and A. G. Guy, Acta. Met. 13 (1965) 957.

22. N. F. Mott, J. Inst. Met. 60 (1937) 267.

23. R. Labusch, phys. stat. sol. 3 (1963) 1661.

24. P. Wilkes, Acta. Met. 16 (1968) 863.

25. P. Wilkes and H. Hillel, Proc. Manchester Conf. on Phase Trans. 1968.

26. R. P. Jewett and D. J. Mack, J. Inst. Met. 92 (1963/4) 59.

27. S. Matsuo and L. M. Clarebrough, Acta. Met. 11 (1963) 1195.

28. H. Warlimont, Z. Metallk. 60 (1969) 195.

29. M. Hansen and K. Anderko (I), R. P. Elliott (II), F. A. Shunk (III), Constitution of Binary Alloys, McGraw-Hill, New York, 1958, 1965, 1969.

30. A. J. Bradley and A. H. Jay, Proc. Roy. Soc. London A 136 (1932) 210.

31. D. Harker, J. Chem. Phys. 12 (1944) 315.

32. R. W. Newman and J. J. Hren, Phil. Mag. 16 (1967) 211.

33. A. S. Kagan, V. A. Somenkov and Ya. S. Umanskii, Kristallographiya 5 (1960) 4.

34. J. C. Fisher, Acta. Met. 2 (1954) 9.

35. P. A. Flinn, Acta. Met. 6 (1958) 631.

36. P. A. Flinn in "Strengthening Mechanisms in Solids," ASM Seminar, Metals Park, Ohio, 1962.

37. P. S. Rudman, Acta. Met. 12 (1964) 1381.

38. G. Kostorz, Z. Metallk. 59 (1968) 941.

39. Ye. N. Vlasova, Fiz. Metal. Metalloved. 23, 5 (1967) 886; Phys. Met. Metallogr. 23, 5 (1967) 113.

40. W. C. Leslie and R. J. Sober, ASM Trans. Quart. 60 (1967) 99, 459.

41. M. F. Ashby and L. M. Brown, Phil. Mag. 8 (1963) 1649.

42. W. L. Bell, D. M. Maher and G. Thomas,"Nature of Small Defect Clusters," HMSO 314, 1966.

43. M. Ruhle, phys. stat. sol. (1967) 263, 279.

44. L. E. Tanner, P. C. Clapp and R. S. Toth, Mat. Res. Bull., 3 (1968) 855.

45. S. S. Rao and T. R. Anantharaman, Z. f. Metallkunde 60 (1969) 312.

46. A. Kussmann und H. Wollenberger, Z. f. Metallkunde 50 (1959) 94.

47. P. C. Clapp and S. C. Moss, Phys. Rev. 142 (1966) 418; 171 (1968) 754, 764.

48. B. G. LeFevre, Ph. D. dissertation, University of Florida, 1966.

49. E. Hornbogen and M. Roth, Z. f. Metallkunde 58 (1967) 842.

50. A. J. Ardell and R. B. Nicholson, Acta Met. 14 (1966) 1295; J. Phys. Chem. Sol. 27 (1966) 1793.

51a. I. Pfeiffer, Z. f. Metallkunde 56 (1965) 465.

51b. P. Wilkes, Acta Met. 16 (1968) 153.

52. P. B. Hirsch, a. Howie, R. B. Nicholson, D. W. Pashley, M. J. Whelan, Electron Microscopy of Thin Crystals, Butterwurths, London, 1965.

53. J. E. Hilliard, Trans. AIME 224 (1962) 906.

54. L. E. Tanner, Phil. Mag. 14 (1966) 111.

55. P. Okamoto and G. Thomas, to be published.

56. S. C. Moss in "Local Atomic Arrangements Studied by X-Ray Diffraction," AIME Met. Soc. Conf. 36, Gordon and Breach, 1966.

57. K. Sato, D. Watanabe, S. Ogawa, J. Phys. Soc. Jap. 17 (1962) 1647.

58. H. Raether, Z. angew. Phys. 4 (1952) 53.

59. D. Watanabe, J. Phys. Soc. Jap. 14 (1959) 436.

60. D. Watanabe and P. M. J. Fisher, J. Phys. Soc. Jap. 20 (1965) 2170.

61. R. L. Fleischer, Acta Met. 9 (1961) 996; 11 (1963) 203; 14 (1966) 1867; in The Strengthening of Metals, D. Peckner ed., Reinhold, New York, 1964.

62. P. Haasen in Proc. of the Conf. on the Strength of Metals and Alloys, Tokyo, 1967.

63. V. Gerold and H. Haberkorn, phys. stat. sol. 16 (1966) 675.

64. H. Gleiter, Z. f. Metallkunde 58 (1967) 99.

65. H. Gleiter and E. Hornbogen, phys. stat. sol. 12 (1965) 235.

66. M. J. Marcinkowski and H. Chessin, Phil. Mag. 10 (1964) 837.

67. G. E. Lakso and M. J. Marcinkowski; private communication.

68. H. J. Leamy, Ph. D. Thesis, Iowa State University, 1967.

69. A. H. Cottrell, "Dislocations and Plastic Flow in Crystals," Clarendon, London, 1953.

70. G. Schanz and H. Warlimont, to be published.

Table 1

Experimental observations on short range ordered alloys

| | Cu-Al | Fe-Al | Ni-Mo | References |
|---|---|---|---|---|
| Apparent average distance of strain centres, D (Å) | ≃ 130 | 100 - 200 | | 4, 7 |
| Apparent diameter of ordered regions, d (Å) | 21; 10 - 20 | < 70; ≃ 50; 10 - 20 | ≃ 12; ≃ 10 | 4, 7, 9 this work |
| Approximate direction of streaking in electron diffraction patterns | <110>,<112> | <110>,<112> | | 4, 7 |
| Extra reflections in diffraction patterns | LPS($c_{Al}$) | $DO_3$ type | a){1,1/2,0} b)$D1_a$ type | 4, 7, 9 this work |

## FIGURE CAPTIONS

Fig. 1. Phase equilibria and ranges of short range order (SRO).

Fig. 2. Ecectron Micrographs of alloys in the state of short range order. Images due to fundamental reflections showing net strain contrast due to finely dispersed strain centres.

(a) Cu-15 at.% Al, 800°C 5.5°/hr 20° C. Dark field, $\vec{g} = (\bar{2}20)$, $\vec{n} \simeq [112]$

(b) Cu-29 .1 at.% Zn, 850°/$H_2O$, 22d 100°C. Bright field, $\vec{g} = (\bar{2}00)$, $\vec{n} \simeq [001]$

(c) Fe-15.5 at.% Al, 1380°/$H_2O$, 1 h 300°C. Bright field, $\vec{g} = (1\bar{1}0)$, $\vec{n} \simeq [111]$

(d) Ni-20.2 at.% Mo, 1100°C/ice brine. Dark field, $\vec{g} = [1\bar{1}1]$

Fig. 3. Electron micrographs of alloys in the state of short range order. Direct images of regions of a high degree of order and/or clustering.

(a) Fe-18.7 at.% Al, 1380°/$H_2O$, i w 300°C. Dark field $\vec{g} = (111)_{DO_3}$

(b) Ni-20.2 at.% Mo, 1100°C/ice brine. Dark field $\vec{g} = \{1,1/2,0\} + (\bar{1}10)_{bct}$

Fig. 4. Field ion micrographs of Ni - 20.2 at.% Mo, 1100°C/ice brine.

(a) As quenced

(b) Aged 10 min. 650°C

Fig. 5. Electron diffraction patterns of alloys in the state of short range order showing the characteristic broadening of fundamental reflections

(a) Cu-15.0 at.% Al, 500°/$H_2O$, 1w 160°C. $\vec{n} = [110]$

(b) Cu-34.0 at.% Zn, 850°/$H_2O$, 1w 200°C. $\vec{n} = [001]$

(c) Fe-17.8 at.% Al, 1380°/$H_2O$, 1w 300°C. $\vec{n}$ = [001]

Fig. 6. Electron diffraction patterns of alloys in the state of short range order showing extra reflections.

(a) Fe-17.8 at.% Al, 1380°/$H_2O$, 1h 300°C. $\vec{n}$ = [001]

(b) Cu-17.0 at.% Al, 500°/$H_2O$, 1w 160°C. $\vec{n}$ = [110]

Fig. 7. Electron diffraction patterns of Ni-20.2 at.% Mo, 1100°C/ice brine, $\vec{n} = [121]_{fcc}$

(a) As quenched

(b) Aged 10 min. at 650°C

(c) Aged 10 sec. at 750°C

Fig. 8. Stress-strain curves of quenched and aged Fe-Al alloys

Fig. 9. $\sigma_{0.1}$ proof stress of quenched and aged Fe-Al alloys

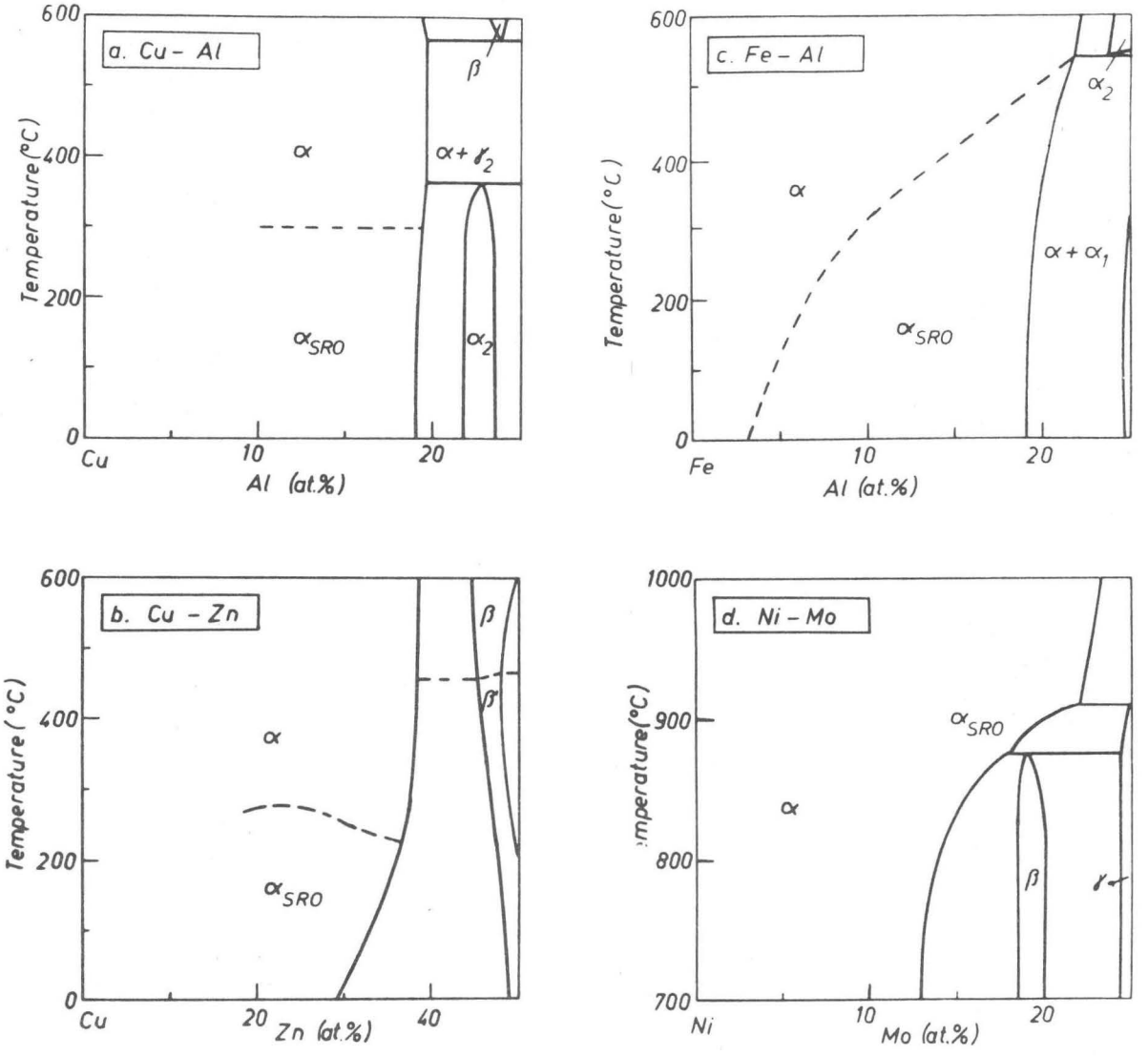


*Fig 1 Phase equilibria and ranges of short range order (SRO)*

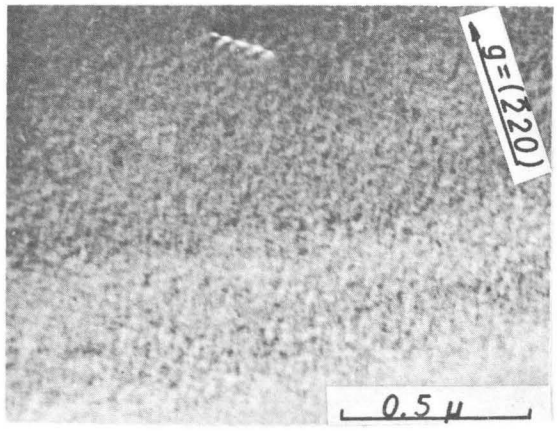


a) Cu-15 at.% Al, 800°C 5,5°/hr 20°C. Dark field, $\vec{g}$ = (220), $\vec{n}$ = [112]

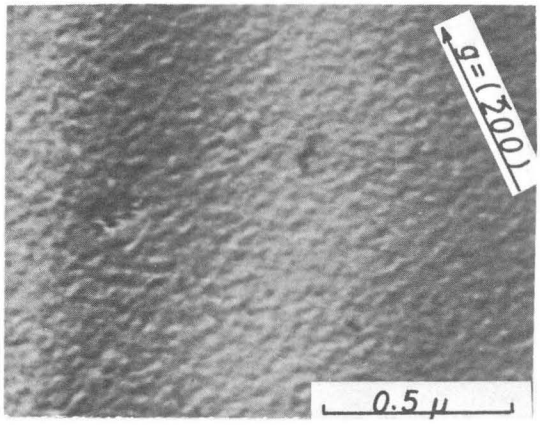


b) Cu-29.1 at.% Zn, 850°/$H_2O$, 22d 100°C. Bright field, $\vec{g}$ = ($\bar{2}$00), $\vec{n}$ = [001]

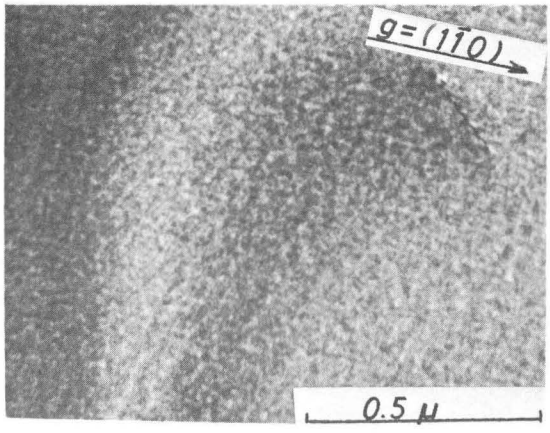


c) Fe-15.5 at.% Al, 1380°/$H_2O$, 1 h 300°C. Bright field, $\vec{g}$ = (1$\bar{1}$0), $\vec{n}$ = [111]

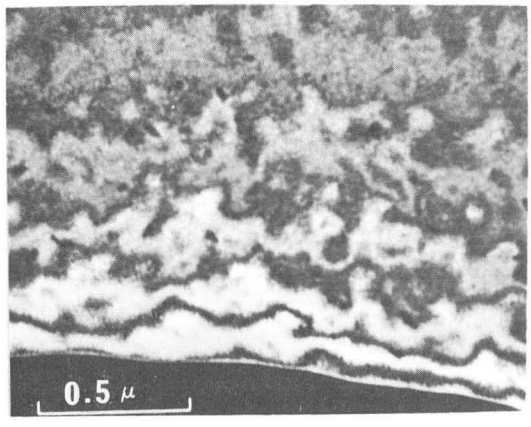


d) Ni-20.2 at.% Mo, 1100°C/ice brine. Dark field, $\vec{g}$ = [1$\bar{1}$1]

XBB 701-251

Fig. 2. Electron micrographs of alloys in the state of short range order. Images due to fundamental reflections showing net strain contrast due to finely dispersed strain centres.

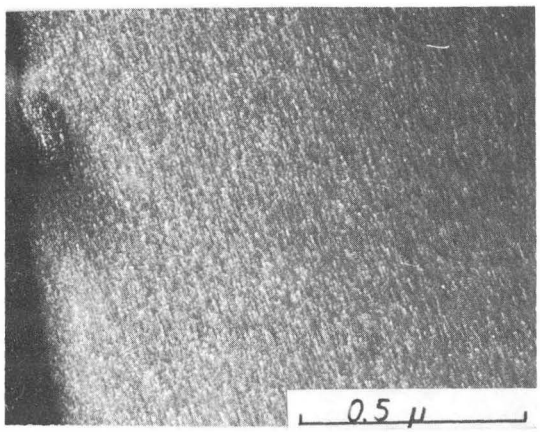


a) Fe-18.7 at.% Al, 1380°/$H_2O$, 1 w 300°C. Dark field $\vec{g} = (111)_{DO_3}$

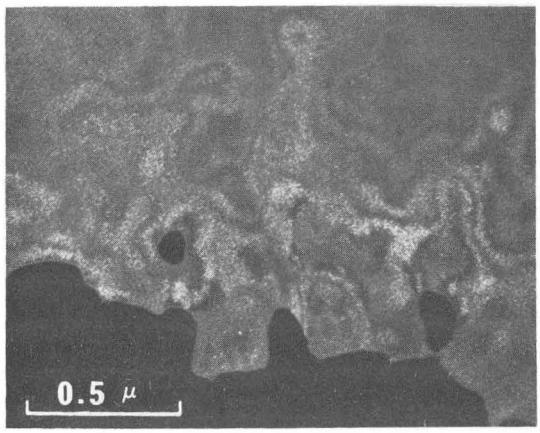


b) Ni-20.2 at.% Mo, 1100°C/ice brine. Dark field $\vec{g} = \{1,1/2,0\} + (\bar{1}10)_{bct}$

XBB 701-250

Fig. 3. Electron micrographs of alloys in the state of short range order. Direct images of regions of a high degree of order and/or clustering.

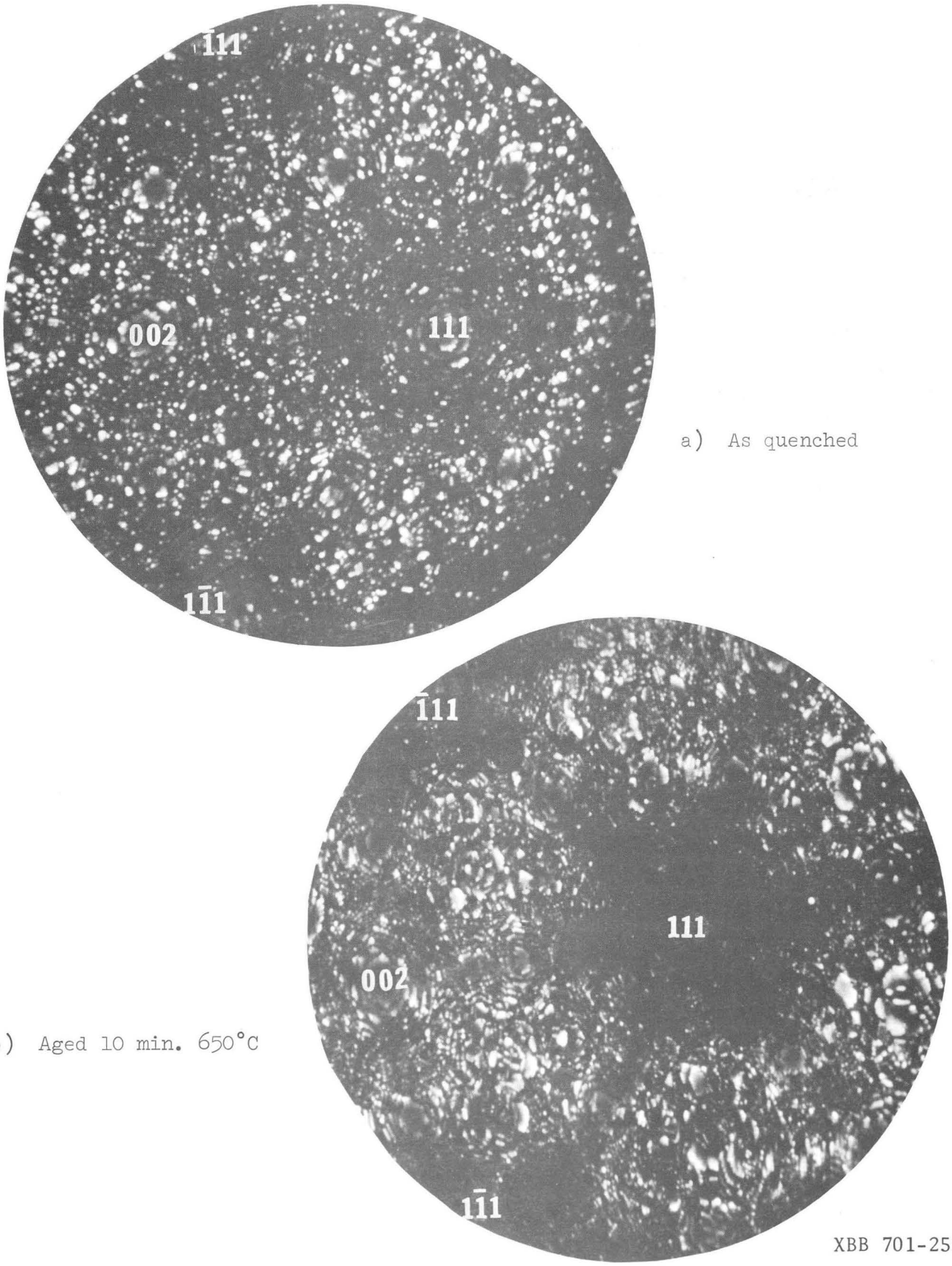


Fig. 4. Field ion micrographs of Ni-20.2 at.% Mo, 1100°C/ice brine.

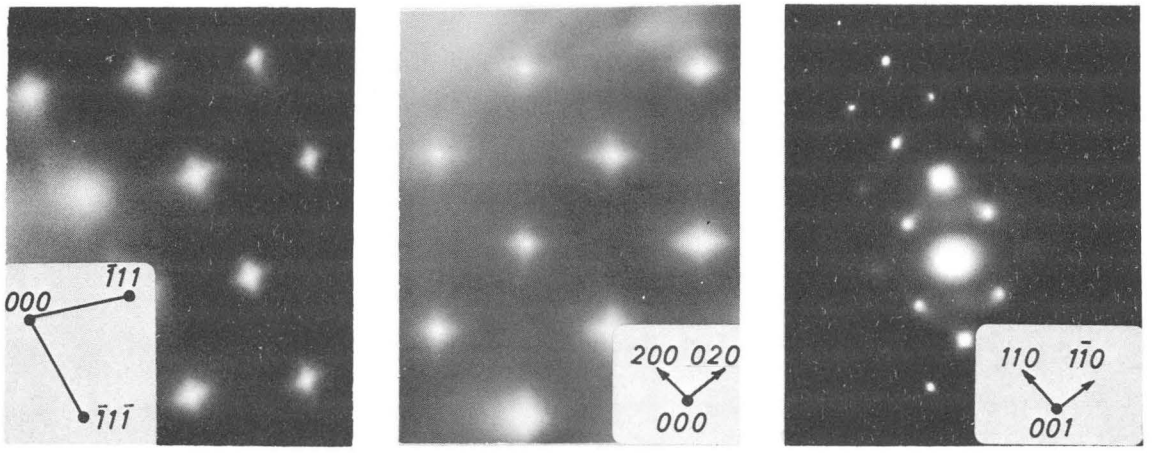


a) Cu-15.0 at.% Al, $500°/H_2O$, 1 w 160°C. $\vec{n} = [1\bar{1}0]$

b) Cu-34.0 at.% Zn, $850°/H_2O$, 1 w 200°C. $\vec{n} = [00\bar{1}]$

c) Fe-17.8 at.% Al, $1380°/H_2O$, 1 w 300°C. $\vec{n} = [00\bar{1}]$

XBB 701-253

Fig. 5. Electron diffraction patterns of alloys in the state of short range order showing the characteristic broadening of fundamental reflections.

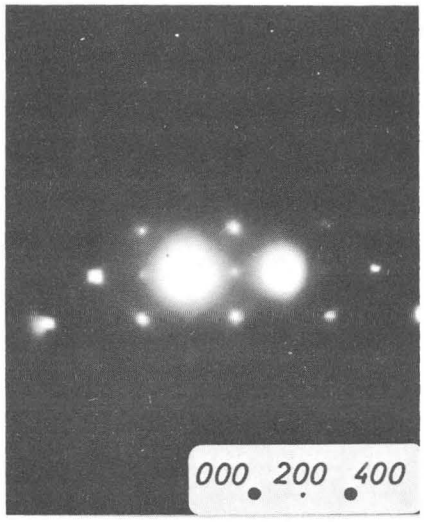


a) Fe-17.8 at.% Al, 1380°/$H_2O$, 1 h 300°C. $\vec{n}$ = [001]

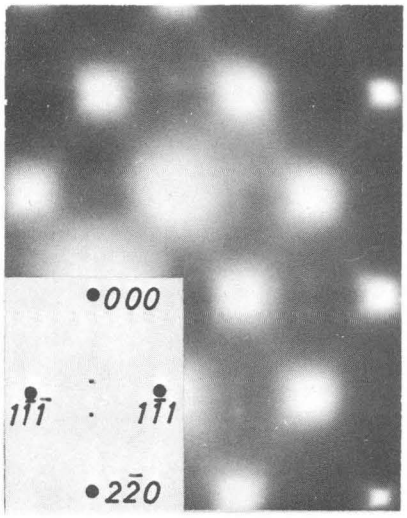


b) Cu-17.0 at.% Al, 500°/$H_2O$, 1 w 160 C. $\vec{n}$ = [110]

XBB 701-252

Fig. 6. Electron diffraction patterns of alloys in the state of short range order showing extra reflections.

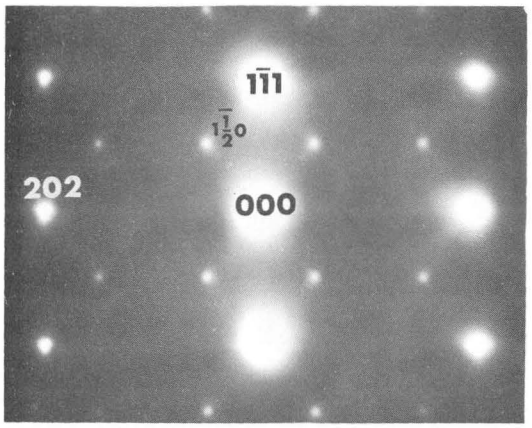


a) As quenched

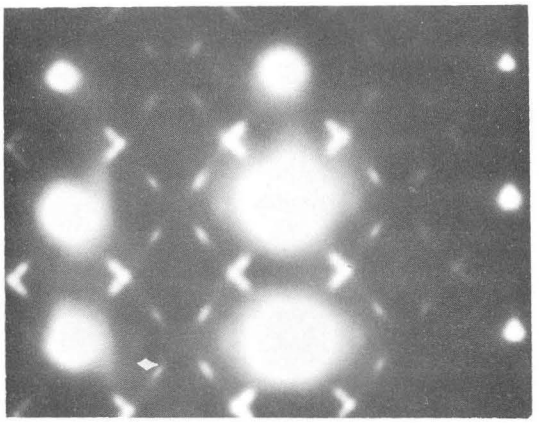

b) Aged 10 min. at 650°C

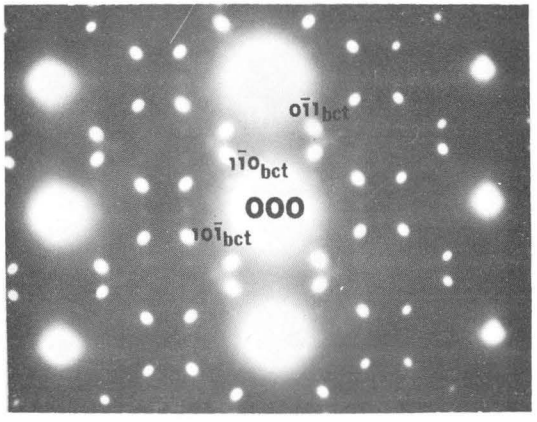


c) Aged 10 sec. at 750°C

XBB 701-254

Fig. 7. Electron diffraction patterns of Ni-20.2 at.% Mo, 1100°C/ice brine, $\vec{n} = [121]_{fcc}$

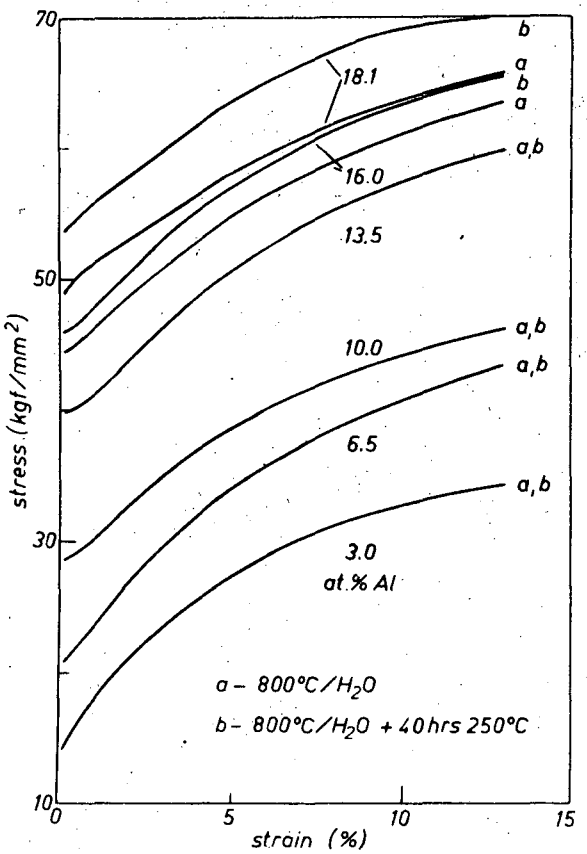


Fig.8 Stress-strain curves of quenched and aged Fe-Al alloys

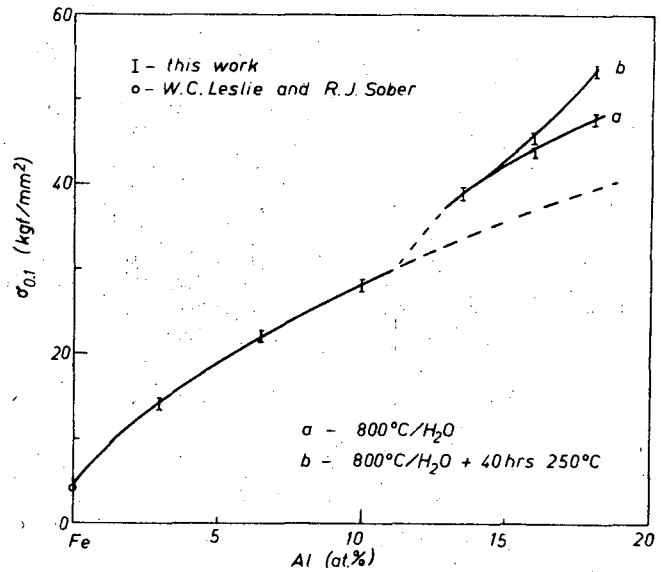


Fig.9 $\sigma_{0.1}$ proof stress of quenched and aged Fe-Al alloys

TECHNICAL INFORMATION DIVISION
LAWRENCE RADIATION LABORATORY
UNIVERSITY OF CALIFORNIA
BERKELEY, CALIFORNIA 94720